Sensitivity of Detonation Re-initiation at a Back-Facing step to Transverse Waves

Yaroslava Poroshyna[1], Gaby Ciccarelli[1], Shem Lau-Chapdelaine[1,2]
[1] – Queen's University, [2] – Royal Military College
Kingston, Ontario, Canada

1 Introduction

Detonation failure due to diffraction and reinitiation after a step change in cross-section area is an important problem to study, both for practical and theoretical reasons. A canonical geometry to study this phenomenon is a back-facing step where reinitiation occurs due to shock reflection on the floor after the step. Most studies on detonation re-initiation focused on identifying specific mechanisms, primarily through experimental and numerical methods. The Mach stem and associated flow structure that form at the bottom wall were suggested to play a key role in detonation initiation, independent of the initial detonation cell structure [1-4]. Later numerical 2D studies highlighted the role of transverse waves and their interaction with burned and unburned gas interfaces behind the incident shock, as well as the interaction of the reflected shock at the bottom wall, as critical mechanisms for detonation re-initiation [5]. In wide channels with negligible losses to the channel walls, the 3D effects were found to be important leading to detonation re-initiation through the collision of descending transverse waves and lateral waves propagating across the channel width at the bottom wall [6]. In a narrow channel, where losses are significant and a single lateral wave is present, detonation may also re-initiate through the interaction of the reflected shock with a descending transverse wave [7].

While these studies provided insight into specific mechanisms of re-initiation, a complimentary approach to understanding detonation dynamics involves a more statistical analysis. The specifics of detonation transmission, re-initiation and failure were demonstrated over a broad range of the opening to the step height ratios in [8]. Yuan et al. demonstrated the role of triple point collisions in detonation re-initiation in 2D numerical simulations of detonation diffracting into an unconfined region, where an obstacle was placed at various downstream positions [9]. Detonation successfully re-initiated when the obstacle aligned with the trajectories of descending triple points. In the current study, we systematically investigate how the landing positions of the triple points affect the detonation re-initiation at the bottom wall of a back-facing step by shifting the position of the step relative to the incident detonation structure. For a regular cell structure mixture, 2D numerical simulations results are compared with narrow- and wide-channel experiments [6, 7] where the incident detonation structure varied stochastically relative to the step.

2 Mathematical model

Correspondence to: 22hw13@queensu.ca

The mathematical model is based on the 2D inviscid Euler equations with perfect gas model, augmented by a two-step kinetic model for chemical reactions [10]:

$$\frac{\partial \rho\lambda_i}{\partial t}+\frac{\partial \rho u_x\lambda_i}{\partial x}+\frac{\partial \rho u_y\lambda_i}{\partial y}=-H(\lambda_i)K_i\rho e^{-\frac{E_a}{RT}}, \qquad \frac{\partial \rho\lambda_r}{\partial t}+\frac{\partial \rho u_x\lambda_r}{\partial x}+\frac{\partial \rho u_y\lambda_r}{\partial y}=\big(1-H(\lambda_i)\big)K_r\rho(1-\lambda_r)^{\nu},$$

where x and y are the spatial coordinates, t is time, ρ is density, u is velocity, p is pressure. Indicies "i" and "r" denote the induction and reaction zones, respectively. λ is the progress variable and K is the rate constant in the respective zones, ν is the reaction order. $H(\lambda_i)$ is the Heaviside function that switches to the reaction zone equation if the induction zone is over. Procedure of matching the Chapman-Jouguet (CJ) Mach number M_{CJ}, the ratio of specific heats γ and the heat release Q/RT_1 is described in [10].

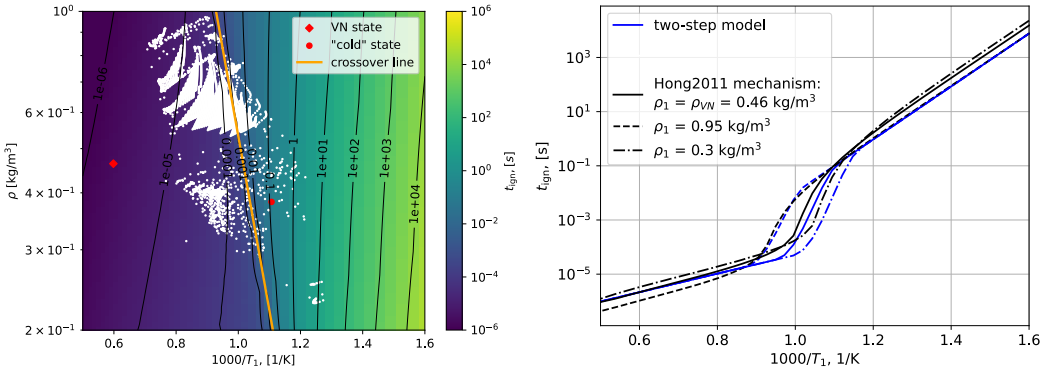

(a) (b)

Figure 1. The constant volume combustion results for different initial densities and temperatures in $2H_2+O_2+2Ar$ [11], [12]: a) ignition time values, the white dots are the states in the unreacted gas behind the shock reflected at the bottom wall. The orange line is the fitted line in the (T, ρ) space where E_a is the largest for each density. b) the ignition times, the black lines denote the results calculated with the detailed chemistry, the blue lines denote the results calculated with the current two-step chemistry model.

It is well known that hydrogen has a crossover temperature range where there is a shift in the ignition time, see Figure 1b. Preliminary simulations revealed that the post-shock conditions following the reflection of the incident shock at the bottom wall, shown by white dots in Figure 1a, lie within this crossover region. Consequently, we employed distinct activation energies E_a and rate constants K_i in the induction zone to match the constant-volume ignition times t_{ign} on either side of the crossover region (orange line in Figure 1) in the temperature-density (T, ρ). The von Neumann state (VN) was selected as a representative point to the left of the crossover line, while one of the states among the white dots in Figure 1a was chosen as a point to the right. Smooth functions (1) and (2) were used to fit the E_a and K_i values, respectively, between the two solutions:

$$\tilde{E}_a=\frac{E_a}{RT_1}=\begin{cases}\tilde{E}_{a,VN}, \\ \dfrac{\tilde{E}_{a,cold}-\tilde{E}_{a,VN}}{2}\,sin\left(A\left(\dfrac{1}{T}-\dfrac{1}{T_{crit}}\right)\right)+\dfrac{\tilde{E}_{a,cold}+\tilde{E}_{a,VN}}{2}, \\ \tilde{E}_{a,cold}, \end{cases} \tag{1}$$

$$K_i=\begin{cases}K_{i,VN}, \\ exp\left(\dfrac{\ln K_{i,VN}-\ln K_{i,cold}}{2}\,sin\left(A\left(\dfrac{1}{T}-\dfrac{1}{T_{crit}}\right)\right)+\dfrac{\ln K_{i,VN}+\ln K_{i,cold}}{2}\right), \\ K_{i,cold}, \end{cases} \tag{2}$$

$$A(\rho)=\frac{\pi}{x_2-x_1}, \quad x_1(\rho)=(1-k)\frac{1}{T_{crit}}, \quad x_2(\rho)=(1+k)\frac{1}{T_{crit}}, \quad \frac{1}{T_{crit}}(\rho)=a\ln\rho+b.$$

to implement the crossover behaviour and link both regions. Figure 1b shows the simplified chemical model accurately represents the detailed chemistry constant volume explosion ignition time over the relevant range of temperatures and densities, including the crossover behavior. All parameters used in the numerical study are summarized in Table 1. The fitting parameters in (1) and (2) are $a = -0.0341$, $b = 0.3645$.

Table 1. The model parameters used in the current study

p_1, kPa	T_1, K	γ	M_{CJ}	Q/RT_1	$\tilde{E}_{a,VN}$	$\tilde{E}_{a,cold}$	$K_{i,VN}$	$K_{i,cold}$	K_r	ν	k
10	300	1.3974	4.896	16.1434	26.314	75.0	130.575	$1.27 \cdot 10^6$	0.61	0.5	0.08

3 Numerical domain

The non-steady calculations were carried out using the finite-volume computational package mg developed by Falle et al. [13-15]. This package features a second-order accurate exact Godunov scheme to handle the convective terms. At t = 0, a ZND profile is specified at the left end of the channel, see Figure 2. Over time, the detonation cellular structure developed in the channel and diffracts at the back-facing step. The boundary conditions for the top, bottom and right sides of the computational domain are symmetrical, and CJ parameters are specified at the left boundary. The solver utilizes adaptive mesh refinement with the finest resolution of 21 grid cells per induction length Δ_i (higher resolution gave a similar number of cells per channel height). The induction length (Δ_i) was calculated to be 0.566 mm for the chosen set of parameters using the method in [11].

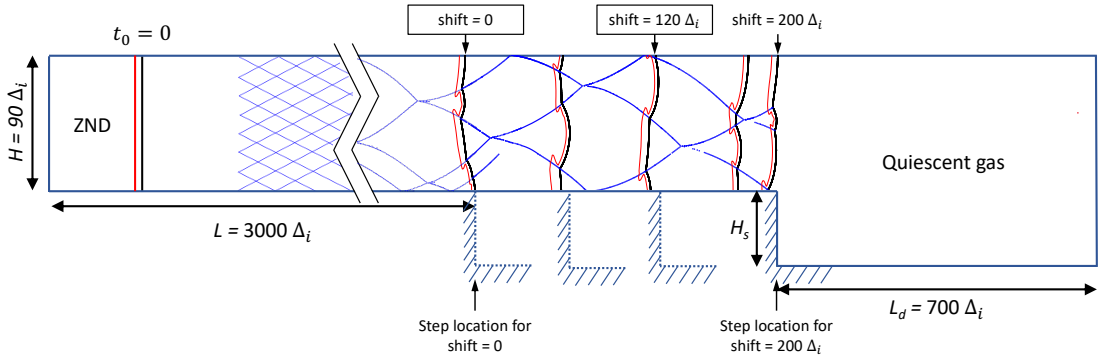

Figure 2. The setup of numerical calculations.

4 Results

To evaluate the effect of descending triple points on detonation re-initiation, the incident cellular detonation front was shifted relative to the step in increments of 10 induction lengths to a maximum shift of 200 induction lengths, resulting in 21 simulations with slightly different detonation front structures at the step before diffraction (see Figure 2, the black lines denote the curved shock fronts, and red lines shows the reaction progress, i.e., $\lambda_r = 0.5$. This is equivalent to letting detonation evolve for up to $200\Delta_i$ more before it starts diffracting.

The shock pressure and shock velocity along the bottom wall after the step across all simulations are plotted in Figure 3, with two cases highlighted in red and blue corresponding to no shift and a shift of the step of $120\Delta_i$, respectively. The diffracting detonation decouples and the shock initially undergoes regular reflection on the bottom wall. The shock pressure rises and then gradually decreases following the formation of a Mach stem. The shock front velocity along the bottom wall, plotted in Figure 3b, is high during regular reflection as it represents the contact point velocity, and decreases as the shock reflection progresses. The arrival of descending transverse shocks at the wall result in pressure and

velocity spikes followed by decay to the CJ condition. The reflection of transverse waves also cause local ignitions at the bottom wall that generates a pressure wave that overtakes and amplifies the leading shock, observed in the blue signal at $x = 200\Delta_i$ in Fig. 3a. Taking the median between all simulations, the effect of transverse wave collisions is smoothened, and a gradual increase of median shock pressure to the theoretical VN pressure and above it. The median from the experiments (cyan curve in Figure 3b) shows the behaviour similar to the median calculated from simulations, except that the VN state is surpassed closer to the step in experiments. Later, the median pressure decreases settling to the VN value again. More spikes appear in both Figure 3a and Figure 3b at $x > 500\Delta_i$, that correspond to the generation of new transverse waves at the detonation front propagating along the bottom wall of what appears to be essentially a quasi-steady detonation. The formation of new cells may be observed in Figures 4a and 4b that show the shock pressure history in the channel for the highlighted cases.

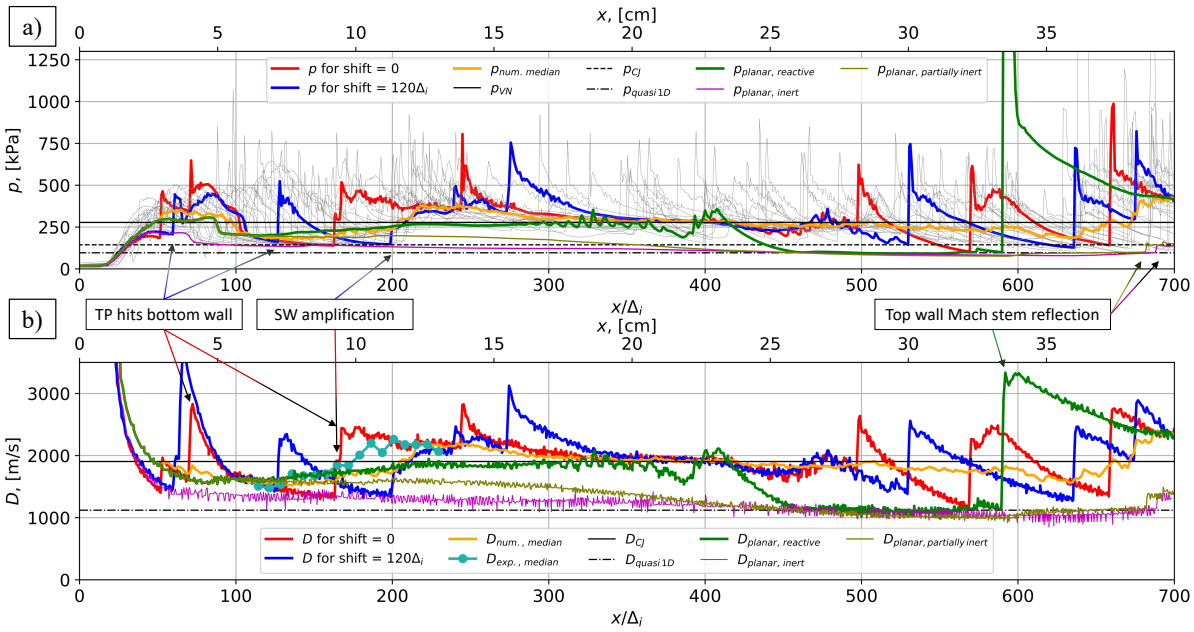

Figure 3. The pressure behind the leading shock front (a) and the velocity of the leading shock front (b) at the bottom wall for different shifts. The horizontal axis is the distance from the step. Grey thin lines denote the values for all numerical test cases except for “shift = 0” and “shift = $120\Delta_i$”.

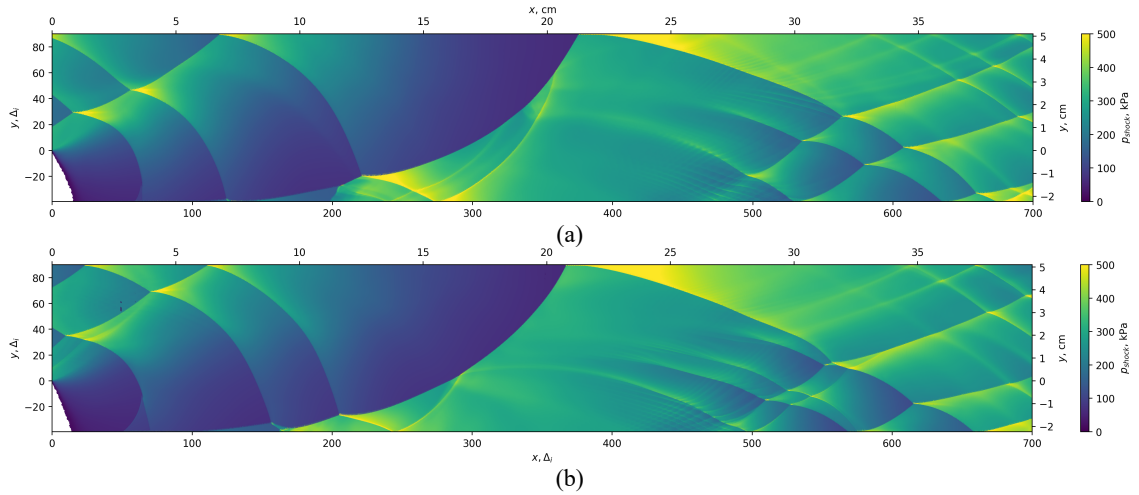

Figure 4. History of pressure behind the leading shock front: a) case "shift = $120\Delta_i$"; b) case “shift = 0” in Figures 2, 3.

To assess the effect of the transverse waves on detonation re-initiation, the diffraction of an initially planar ZND wave (i.e., no transverse waves) was simulated at the back-facing step (green line in Figure 3). The shock pressure and shock velocity along the bottom wall in the planar case are similar to the median curve, not perturbed by the spikes due to the transverse waves. The planar case approaches the theoretical VN value as well; however, no new transverse waves appear establishing a cellular structure. Subsequently the detonation decouples into a shock and trailing flame, resulting in a drop in shock pressure. Detonation initiation occurs at the top wall instead. The large spike at $x \approx 590\Delta_i$ is related to reflection of the detonation from the top wall. The value, that the planar case decreases to, after the shoc-flame decouples is predicted using a non-reactive variation of the quasi-1D model described in [16] (with a quenched flame). If the reactions are artificially turned off when the ZND wave is about to diffract (purple line in Figure 3), or when the reactive ZND wave has reflected at the bottom wall, but the reactions haven't started yet (olive line in Figure 3), then the shock pressure and velocity also gradually approach the values provided by the quasi-1D model.

Table 2 shows the re-initiation distances for the numerical simulations presented in Figure 3, including the shifted cellular detonation, the planar ZND, and the quasi-1D model. Also tabulated is experimental data from the wide [6] and narrow [7] channels, that include 16 experiments performed at the same initial pressure where the incident detonation front structure changed due to natural stochasticity. In the narrow channel, losses to the side walls result in a significant CJ velocity deficit and a larger cell size. The re-initiation criteria is defined as the point where the detonation begins propagating at the CJ velocity along the bottom wall (or when the shock pressure oscillates around the VN pressure). The quasi-1D model predicts the largest re-initiation distance in the absence of any wave reflections at the bottom wall highlighting their importance to the phenomenon. In contrast, 2D numerical simulations show re-initiation distances comparable to those observed in narrow-channel experiments conducted at the same initial pressure. In the case of a initially planar ZND detonation, although the mixture is ignited and the shock pressure reaches p_{VN}, the lack of transverse waves to promote detonation re-initiation (as for the cellular detonations) leads to detonation failure at the bottom wall. The shortest re-initiation distances are observed in 3D experiments conducted in a wide channel under the same initial conditions. This can be attributed to the broader range of parameters in 3D, including higher temperatures at collision points — not only where descending transverse waves interact with the bottom wall but also where lateral waves collide [17].

Table 2. The re-initiation distances in different test cases (p_1 = 10 kPa).

Tests description	Geometry	Cell height, λ, cm	Number of descending TW	Number of lateral TW	Re-initiation distance, cm
Quasi-1D model	Quasi-1D	-	0	0	~200
Planar ZND simulation	2D, no losses	-	0	0	~22
21 cellular simulations	2D, no losses	2.5-3.4	3-5	0	9.5 – 13
16 experiments [7]	2D, w = 12.5 mm	2-3.4	3-5	1	5.2 – 10.6
5 experiments [6]	3D, w = 75 mm	2	5	6-7	5.3 – 7.1

The slight variation in initial conditions leads to different re-initiation mechanisms in both numerical simulations and experiments. In narrow channels, detonation re-initiation can occur through transverse wave collisions or a transverse wave interacting with a reflected shock behind the leading front, which initiates detonation in the unburnt region [7]. This contrasts with wide channels where the re-initiation mechanism remains consistent at a given initial pressure and it is limited to wave collisions propagating at the shock front in the transverse and lateral directions [6]. The numerical simulations also show that re-initiation happens through collisions of descending triple points with the bottom wall. Some incident cellular structures are favorable for re-initiation just due to the triple points (Figure 4b), and some also rely on the ignition at the triple points locations which causes waves amplification that catch up to the shock front (Figure 4a), also reported in [4]. This variety in re-initiation mechanisms for the same

geometry, initial pressure but slightly different incident shock structures highlights sensitivity of detonation re-initiation to lateral and transverse waves.

5 Conclusion

This study examined the role of transverse waves in detonation re-initiation after diffraction at a back-facing step. Through numerical simulations, we observed that the re-initiation mechanisms depend on the interaction of triple points with the bottom wall, with the process transitioning from shock wave amplification-dominated mechanisms to those driven by descending transverse waves associated with the initial detonation cellular structure. In both 2D numerical simulations and experiments (inherently 3D), there is a large variation in re-initiation distances and mechanisms for very similar initial conditions; this highlights the important role played by transverse waves in the re-initiation of detonation.

Acknowledgements

The authors would like to thank Sam Falle, whose numerical code mg made the simulations possible. This project was funded by the Natural Science and Engineering Research Council of Canada (NSERC) by grants to G. Ciccarelli and S. SM. Lau-Chapdelaine. This research was enabled in part by support provided by the Digital Research Alliance of Canada.

References

[1] Ohyagi S, Obara S, Hoshi S, Cai P, Yoshihashi T. (2002). Diffraction and re-initiation of detonations behind a backward-facing step. Shock Waves 12:221–226.
[2] Bhattacharjee RR, Lau-Chapdelaine SSM, Maines G, Maley L, Radulescu MI. (2013). Detonation reinitiation mechanism following the Mach reflection of a quenched detonation. Proc. Combust. Inst. 34(1):1893–1901.
[3] Oran ES, Boris JP, Jones DA, Sichel M. (1993). Ignition in a complex Mach structure. Prog. Astro. Aero. 153:241–252.
[4] Lv Y, Ihme M. (2015). Computational analysis of re-ignition and re-initiation mechanisms of quenched detonation waves behind a backward facing step. Proc. Combust. Inst. 35:1963–1972.
[5] Floring G, Peswani M, Maxwell B. (2023). On the role of transverse detonation waves in the re-establishment of attenuated detonations in methane–oxygen. Combustion and Flame 247:112497.
[6] Poroshyna Y, Loiseau J, Lau-Chapdelaine SSM, Ciccarelli G. (2024). 3D effects of detonation re-initiation after diffraction at a back-facing step. Proc. Combust. Inst. 40:105325.
[7] Poroshyna Y, Loiseau J, Lau-Chapdelaine S, Ciccarelli G. (2025). Mechanisms of detonation re-initiation after a back-facing step in a narrow channel. Submitted to ICDERS, Ottawa, Canada.
[8] Hu J, Cheng J, Zhang B. (2023). The diffraction and re-initiation behavior of detonation wave in premixed H2–O2–Ar mixture, Phys. Fluids 35:095109.
[9] Yuan XQ, Yan C, Zhou J, Ng HD. (2021). Computational study of gaseous cellular detonation diffraction and re-initiation by small obstacle induced perturbations. Phys. Fluids 33:047115.
[10] Borzou B. (2016). The Influence of Cellular Structure on the Dynamics of Detonations with Constant Mass Divergence. PhD thesis, University of Ottawa. P. 139.
[11] Goodwin DG, Moffat HK, Speth RL. (2016). Cantera: An Object-oriented Software Toolkit for Chemical Kinetics, Thermodynamics, and Transport Processes. [Online]. Available: http://www.cantera.org
[12] Hong Z, Davidson DF, Hanson RK. (2011). An improved H2/O2 mechanism based on recent shock tube/laser absorption measurements. Combustion and Flame 158(4):633–644.
[13] Falle, SAEG. (1991). Self-similar jets. Monthly Notices of the Royal Astronomical Society. 250(3):581–596.
[14] Falle SAEG, Giddings JR. (1992). Body capturing using adaptive Cartesian grids. Numerical methods for fluid dynamics: 335–342.
[15] Falle S, Komissarov S. (1996). An upwind numerical scheme for relativistic hydrodynamics with a general equation of state. Monthly Notices of the Royal Astronomical Society. 278(2):586–602.
[16] Salas MD. (1993). Shock wave interaction with an abrupt area change. Applied Num. Math. 12:239-256.
[17] Paknahad R, Lipkowicz JT, Gaffran N, Wlokas I, Kempf AM, Crane J. (2024). Statistics of detonation confinement: 1D, 2D and 3D simulations in hydrogen–oxygen. Proc. Combust. Inst. 40:105388.